

# Effects of Gravitational Lensing and Companion Motion on the Binary Pulsar Timing

Roman R. Rafikov\*

*CITA, McLenan Physics Labs, 60 St. George St.,  
University of Toronto, Toronto, ON M5S 3H8, Canada*

Dong Lai†

*Department of Astronomy, Cornell University, Ithaca, NY 14853*

(Dated: October 30, 2018)

The measurement of the Shapiro time delay in binary pulsar systems with highly inclined orbit can be affected both by the motion of the pulsar’s companion because of the finite time it takes a photon to cross the binary, and by the gravitational light bending if the orbit is sufficiently edge-on relative to the line of sight. Here we calculate the effect of retardation due to the companion’s motion on various time delays in pulsar binaries, including the Shapiro delay, the geometric lensing delay, and the lens-induced delays associated with the pulsar rotation. Our results can be applied to systems so highly inclined that near conjunction gravitational lensing of the pulsar radiation by the companion becomes important (the recently discovered double pulsar system J0737-3039 may exemplify such a system). To the leading order, the effect of retardation is to shift all the delay curves backward in time around the orbit conjunction, without affecting the shape and amplitude of the curves. The time shift is of order the photon orbit crossing time, and ranges from a second to a few minutes for the observed binary pulsar systems. In the double pulsar system J0737-3039, the motion of the companion may also affect the interpretation of the recent correlated interstellar scintillation measurements. Finally, we show that lensing sets an upper limit on the magnitude of the frame-dragging time delay caused by the companion’s spin, and makes this delay unobservable in stellar-mass binary pulsar systems.

PACS numbers: 95.30.Sf – 95.85.Bh–97.60.Gb–97.60.Jd–97.60.Lf–97.80.-d

## I. INTRODUCTION

Timing study of binary radio pulsars has provided some of the best tests of the general relativity (GR) to date. Among the effects that have been probed in different systems are gravitational redshift, precession of the periastron and orbital decay due to gravitational wave emission. Strong evidence for the geodetic precession – GR manifestation of the spin-orbital coupling of the binary – has been found in several systems (e.g., [1], [2]). In binaries with highly inclined orbits, it has been possible to measure the Shapiro delay caused by the propagation of the pulsar signal in the companion’s gravitational field (e.g., [3], [4], [5]).

In systems that have nearly edge-on orbital orientation, like the recently discovered double pulsar system J0737-3039 [3], one may also look for the effects related to the gravitational bending of the pulsar radio beam as it passes close to the companion around the moment of the pulsar’s superior conjunction ([6], [7], [8], [9]). Light bending modifies the conventional Shapiro delay formula widely used in pulsar timing studies and introduces additional geometric time delay ([6], [8]). Bending also gives rise to a *lens-rotational delay* associated with the rotating beam of the pulsar and induces distortion of the pulse profile shape near conjunction [9].

Our previous studies of the lensing effects in binary pulsar systems ([8], [9]) adopted a “static lens” approximation, in which the companion motion is neglected. Kopeikin & Schafer [10] showed that the orbital motion of the pulsar companion gives rise to a  $v_c/c$  correction ( $v_c$  is the companion velocity) to the conventional Shapiro delay formula and such correction might be observable under some circumstances. The work of [10], however, neglected light bending and thus cannot be applied to the situation where the light ray passes the companion within a few Einstein radii. On the other hand, only for such highly inclined systems are the lensing effects potentially observable ([8], [9]).

In this paper we study the effect of companion motion on the time delays associated with the gravitational light bending near the companion. These include both the lensing corrections to the delays independent of the pulsar spin – Shapiro and geometric delays (see §III), and the lens-rotational time delays (§IV). Our formulae are general and valid in both the “strong lensing” and the “weak lensing” regimes. We also provide a simple and general interpretation of the influence of the lens motion on the behavior of various timing signals in binary pulsar systems (§VI) which has not been previously discussed.

Qualitatively, we expect that near binary conjunction the effect of moving lens amounts to a time shift in various time delay curves. It takes finite amount of time for the pulsar signal to travel across the binary system during which the position of its companion changes. Based on simple geometric considerations, this time shift is  $(M_p/M)a_{\parallel}/c$ , where  $M_p$  is the pulsar mass,  $M$  is the

---

\*Electronic address: rrr@cita.utoronto.ca

†Electronic address: dong@astro.cornell.edu

total mass of the system, and  $a_{\parallel}$  is a separation between binary components projected along the line of sight [see eq. (4)]. In the limit  $M_p \rightarrow 0$  this retardation delay goes to zero since companion does not move. Our explicit calculations and general expressions of various time delays confirm this simple expectation, see §VI.

For completeness, in §V we discuss the effect of frame dragging due to the companion's spin on the time delay. This type of delay was previously investigated by [11], [12], [13], [14], who disregarded light bending in their studies. We incorporate the lensing effect in our calculation of the frame-dragging delay, and show (§VIB) that this delay is unobservable in the binary pulsar systems with stellar mass companions.

## II. LENSING BY MOVING PULSAR COMPANION

Consider a binary system consisting of a pulsar with mass  $M_p$  and a companion with mass  $M_c$  (the total mass is  $M = M_p + M_c$ ). Let  $\mathbf{r}_p, \mathbf{r}_c$  be their position vectors with respect to the binary center-of-mass, and  $\mathbf{R}_p, \mathbf{R}_c$  be their projections on the plane of the sky. We also define  $\mathbf{r} = \mathbf{r}_p - \mathbf{r}_c$  (the position vector of the pulsar relative to its companion),  $r_{\parallel} \equiv -\mathbf{n}_0 \cdot \mathbf{r}$  (the projection of  $\mathbf{r}$  along the line of sight; here  $\mathbf{n}_0$  is the unit vector from the binary barycenter to the observer), and  $\mathbf{R} \equiv \mathbf{R}_p - \mathbf{R}_c = \mathbf{n}_0 \times (\mathbf{r} \times \mathbf{n}_0)$  (the projection of  $\mathbf{r}$  in the sky plane). For a binary orbit characterized by the semimajor axis  $a$ , eccentricity  $e$ , longitude of periastron  $\omega$  and inclination angle  $i$ , we have

$$r = |\mathbf{r}| = a(1 - e^2)/(1 + e \cos \phi), \quad (1)$$

$$r_{\parallel} = r \sin i \sin \psi, \quad (2)$$

$$R = |\mathbf{R}| = r(1 - \sin^2 i \sin^2 \psi)^{1/2}, \quad (3)$$

where  $\psi$  is the true anomaly measured from the ascending node of the pulsar and  $\phi = \psi - \omega$  is the orbital true anomaly measured from the periastron. To describe gravitational lensing of the pulsar signal by its companion, it is also useful to introduce

$$a_{\parallel} = a |\sin i| (1 - e^2)/(1 + e \sin \omega), \quad (4)$$

which is the value of  $r_{\parallel}$  at the superior conjunction of the pulsar ( $\psi = \pi/2$ ).

A photon (radio pulse) emitted by the pulsar at time  $t = t_e$  from the position  $\mathbf{R}(t_e)$  passes through the lens plane at time  $t_l \simeq t_e + r_{\parallel}/c$ . In the absence of light bending, the impact parameter of the ray is

$$\begin{aligned} \mathbf{b}_0 &= \mathbf{R}_p(t_e) - \mathbf{R}_c(t_l) = \mathbf{R}(t_e) + \mathbf{R}_c(t_e) - \mathbf{R}_c(t_l) \\ &\simeq \mathbf{R}(t_e) - r_{\parallel} \frac{\mathbf{V}_c(t_e)}{c} = \mathbf{n}_0 \times \left[ \left( \mathbf{r} - r_{\parallel} \frac{\mathbf{v}_c}{c} \right) \times \mathbf{n}_0 \right] \end{aligned} \quad (5)$$

where  $\mathbf{V}_c \equiv d\mathbf{R}_c/dt = \mathbf{n}_0 \times (\mathbf{v}_c \times \mathbf{n}_0)$  is the projection of the companion velocity  $\mathbf{v}_c$  in the plane of the sky. In

terms of the binary orbital parameters we have

$$\begin{aligned} b_0^2 &= [r \cos \psi - d(\sin \psi + e \sin \omega)]^2 \\ &+ [r \sin \psi \cos i + d \cos i (\cos \psi + e \cos \omega)]^2. \end{aligned} \quad (6)$$

Here, to characterize the effect of lens motion, we have introduced the parameter  $d$  given by

$$d \equiv a_{\parallel} \frac{\Omega_b a_c}{c\sqrt{1 - e^2}} = a_c \frac{\Omega_b a \sin i}{c(1 + e \sin \omega)}, \quad (7)$$

where  $a_c = a(M_p/M)$  is the companion's semi-major axis and  $\Omega_b = (GM/a^3)^{1/2}$  is the binary angular frequency. Note that in eq. (6) and the remainder of the paper, all variables are evaluated at the time of pulse emission  $t = t_e$ .

Because of light bending, the actual impact parameter of the ray (i.e. the minimum-approach distance between the radio beam and the companion),  $b$ , differs from  $b_0$ . The bending angle, including the leading-order correction due to the companion motion, is (e.g., [15], [16])

$$\alpha = \left( 1 - \frac{\mathbf{n}_0 \cdot \mathbf{v}_c}{c} \right) \frac{4GM_c}{c^2 b}, \quad (8)$$

The  $v_c/c$  correction to the classical light-bending formula only slightly affects the value of the companion's Einstein radius, and will be dropped in the remainder of the paper. We are only interested in lensing around the superior conjunction of the pulsar, during which  $b_0 \sim R \ll r_{\parallel} \simeq a_{\parallel}$  is well satisfied. Lensing gives rise to two images (positive and negative) of the source located at  $\mathbf{b}_{\pm} = b_{\pm} \mathbf{b}_0/b_0$  in the plane of the sky with respect to the companion's position. From the lensing equation,  $b - b_0 = \alpha a_{\parallel}$ , we find the impact parameters of the two images:

$$b_{\pm} = \frac{1}{2} \left( b_0 \pm \sqrt{b_0^2 + 4R_E^2} \right), \quad (9)$$

where  $R_E$  is the Einstein radius given by

$$R_E = (2R_g a_{\parallel})^{1/2}, \quad R_g = 2GM_c/c^2. \quad (10)$$

The image amplification  $A_{\pm} = d(b_{\pm}^2)/d(b_0^2)$  is given by the standard expression

$$A_{\pm} = \frac{u^2 + 2}{2u\sqrt{u^2 + 4}} \pm \frac{1}{2}, \quad \text{with } u = b_0/R_E. \quad (11)$$

Clearly, the motion of the companion affects the lensing images only through the "retardation" term in eq. (5), arising from the finite time  $r_{\parallel}/c$  that photons spend traveling between the pulsar and the lens plane of the companion.

## III. GEOMETRIC AND SHAPIRO DELAYS

Lai & Rafikov [8] gave the expressions for the geometric delay and the lensing-corrected Shapiro delay for highly

inclined binary pulsar systems based on the static approximation. Here we revise these expressions taking into account the motion of the companion.

To order  $\mathcal{O}(v_c/c)$ , the expression for the geometric delay assumes the usual form (see Appendix A)

$$(\Delta t)_{\text{geom}} = \frac{R_g}{c} \left( \frac{\Delta b_{\pm}}{R_E} \right)^2, \quad (12)$$

where the image displacement is given by

$$\Delta b_{\pm} = b_{\pm} - b_0 = \frac{1}{2} \left( \pm \sqrt{b_0^2 + 4R_E^2} - b_0 \right). \quad (13)$$

The leading-order  $v_c/c$  correction to  $(\Delta t)_{\text{geom}}$  enters through the expression for  $b_0$  [see eq. (6)]. Compared to the static limit [8] the only difference is in using  $b_0$  instead of  $R$  in eq. (13).

The easiest way to illustrate how the lens motion affects the Shapiro delay is to switch to a reference frame co-moving with the companion [39]. In this frame, the companion's gravitational field is static and the expression for the Shapiro delay derived in [8] [see their eq. (5)] can be used. The expression involves  $r_{\parallel}$  and  $b$ . Because of the aberration of light, the direction of photon propagation in the comoving frame  $\mathbf{n}'$  is given by  $\mathbf{n}' \simeq \mathbf{n}_0 - \mathbf{V}_c/c$ . Thus, instead of  $r_{\parallel}$  one has to use  $r'_{\parallel} = -\mathbf{n}' \cdot \mathbf{r} = r_{\parallel} + \mathbf{R} \cdot \mathbf{V}_c/c$ . Also, the difference between  $b'_{\pm}$  (the impact parameter of the ray in the comoving frame) and  $b_{\pm}$  is proportional to  $(v_c/c)^2$ . Thus, including the leading order  $v_c/c$  correction, the gravitational (Shapiro) delay is given by (cf. eq. (5) of [8])[40]

$$\begin{aligned} (\Delta t)_{\text{grav}} = & - \left( 1 - \frac{\mathbf{n}_0 \cdot \mathbf{v}_c}{c} \right) \frac{R_g}{c} \\ & \times \ln \left[ \sqrt{(r_{\parallel} + \mathbf{R} \cdot \mathbf{V}_c/c)^2 + b_{\pm}^2} - r_{\parallel} - \mathbf{R} \cdot \mathbf{V}_c/c \right] \\ & + \frac{R_g}{c} \ln [a(1 - e^2)]. \end{aligned} \quad (14)$$

Note that the prefactor  $(1 - \mathbf{n}_0 \cdot \mathbf{v}_c/c)$ , which was absent in the original formula of [8], is not captured in our simple analysis given above. A formal derivation of eq. (14) is given in Appendix A.

In the ‘‘weak lensing’’ limit, when  $b_0 \gg R_E$  [or equivalently,  $(\Delta\psi)^2 + (\Delta i)^2 \gg (R_E/a_{\parallel})^2 \sim (v/c)^2$ , where  $\Delta\psi = \psi - \pi/2$  and  $\Delta i = i - \pi/2$ ], we have for the positive image [41],  $\Delta b_+ \simeq R_E^2/b_0 = 2a_{\parallel}(v/c)(R_E/b_0) \ll a_{\parallel}(v/c)$ , where  $v \simeq (GM/a_{\parallel})^{1/2}$ . Thus,  $\mathbf{b}_+ \simeq \mathbf{R} - r_{\parallel}\mathbf{V}_c/c$ . Keeping only terms up to order  $\mathcal{O}(v_c/c)$ , the numerator of the expression inside the logarithm in eq. (14) reduces to  $r - r_{\parallel} - \mathbf{R} \cdot \mathbf{V}_c/c = r + \mathbf{r} \cdot [\mathbf{n}_0 - \mathbf{n}_0 \times (\mathbf{v}_c \times \mathbf{n}_0)/c]$ . As a result, in the absence of lensing, eq. (14) becomes

$$\begin{aligned} (\Delta t)_{\text{grav}} = & - \left( 1 - \frac{\mathbf{n}_0 \cdot \mathbf{v}_c}{c} \right) \frac{R_g}{c} \\ & \times \ln \left[ r + \mathbf{n}_0 \cdot \mathbf{r} - \frac{\mathbf{n}_0 \times \mathbf{v}_c}{c} \cdot (\mathbf{n}_0 \times \mathbf{r}) \right] \\ & + \frac{R_g}{c} \ln [a(1 - e^2)]. \end{aligned} \quad (15)$$

which agrees with the no lensing result obtained in [10] (see also [17]).

Not too far from the binary conjunction, when  $R \simeq a_{\parallel}[(\Delta\psi)^2 + (\Delta i)^2]^{1/2} \ll a_{\parallel}$ , eq. (14) reduces to

$$\begin{aligned} (\Delta t)_{\text{grav}} = & - \left( 1 - \frac{\mathbf{n}_0 \cdot \mathbf{v}_c}{c} \right) \frac{R_g}{c} \ln \left( \frac{b_{\pm}^2 f}{2r_{\parallel}} \right) \\ & + \frac{R_g}{c} \ln [a(1 - e^2)]. \end{aligned} \quad (16)$$

where  $f \simeq 1 - \mathbf{R} \cdot \mathbf{V}_c/(cr_{\parallel}) \simeq 1$ . Note that the regions of validity of the limiting cases described by eqs. (16) and (15) have a significant interval of overlap  $[(v/c)^2 \ll (\Delta\psi)^2 + (\Delta i)^2 \ll 1]$ .

#### IV. LENS-ROTATIONAL DELAYS

Because of light bending of the pulsar signal by the companion, the direction of emission  $\mathbf{n}$  at the pulsar position differs from  $\mathbf{n}_0$ , with the deflection vector  $(\Delta\mathbf{n})_L = \mathbf{n} - \mathbf{n}_0$  given by

$$(\Delta\mathbf{n})_L = \frac{\Delta\mathbf{b}_{\pm}}{a_{\parallel}} = \left( \frac{\Delta b_{\pm}}{b_0} \right) \frac{\mathbf{n}_0 \times [(\mathbf{r} - a_{\parallel}\mathbf{v}_c/c) \times \mathbf{n}_0]}{a_{\parallel}}, \quad (17)$$

where  $\Delta\mathbf{b}_{\pm} = \mathbf{b}_{\pm} - \mathbf{b}_0 = \Delta b_{\pm}(\mathbf{b}_0/b_0)$  [see eqs. (5) and (13)]. Again, we are interested in the lensing effect only around the superior conjunction of the pulsar, so that  $r_{\parallel} \simeq a_{\parallel}$ . Since pulsar signals are due to the beamed emission of the neutron star (as opposed to radial pulsation), such a change in the emission direction gives rise to time delays and pulse profile distortion which depend on the pulsar spin period ([9])[42].

In the following we will use the description of the pulsar spin geometry from [18] (see their Fig. 1) in which the pulsar spin axis  $\mathbf{s}_p$  (the unit vector along the pulsar spin direction) is specified by two angles:  $\zeta_p$  is the angle between  $\mathbf{s}_p$  and the light-of-sight vector  $\mathbf{n}_0$ , and  $\eta_p$  is the angle between the ascending node of the orbit and the projection of  $\mathbf{s}_p$  on the sky plane.

##### A. Longitudinal Time Delay

Variation of the emission direction  $(\Delta\mathbf{n})_L$  causes a shift in the equatorial *longitude*  $\Phi$  of the emission direction in the corotating frame of pulsar (counted in the direction of rotation):

$$\Delta\Phi = \frac{(\Delta\mathbf{n})_L \cdot (\mathbf{s}_p \times \mathbf{n}_0)}{|\mathbf{s}_p \times \mathbf{n}_0|^2}. \quad (18)$$

This longitudinal shift corresponds to a change of the emission phase, leading to a *longitudinal* time delay  $(\Delta t)_L = \Delta\Phi/\Omega_p$  ( $\Omega_p$  is the angular frequency of the pulsar; the time delay is positive for signal arriving later). This delay is independent of the specific emission pattern

(as long as it is rigidly rotating around  $\mathbf{s}_p$ ) and is given by (cf. [9])

$$(\Delta t)_L = \left( \frac{\Delta b_{\pm}}{b_0} \right) \frac{(\mathbf{r} - a_{\parallel} \mathbf{v}_c/c) \cdot (\mathbf{s}_p \times \mathbf{n}_0)}{\Omega_p a_{\parallel} |\mathbf{s}_p \times \mathbf{n}_0|^2} \quad (19)$$

$$(\Delta t)_L = - \left( \frac{\Delta b_{\pm}}{b_0} \right) \times \left[ \left( \frac{r}{a_{\parallel}} \right) \frac{\sin \eta_p \cos \psi - \cos i \cos \eta_p \sin \psi}{\Omega_p \sin \zeta_p} - \left( \frac{d}{a_{\parallel}} \right) \frac{\sin \eta_p (\sin \psi + e \sin \omega) + \cos i \cos \eta_p (\cos \psi + e \cos \omega)}{\Omega_p \sin \zeta_p} \right], \quad (20)$$

where  $b_0$  is given by eq. (6). Setting  $d = 0$  recovers the expression for the longitudinal lens-rotational delay obtained in [9] under static approximation.

### B. Pulse Profile Variation and Latitudinal Time Delay

Variation of the pulse emission direction  $(\Delta \mathbf{n})_L$  also results in the change of *colatitude*  $\zeta$  of the emission vector:

$$\begin{aligned} (\Delta \zeta)_L &= - \frac{\mathbf{s}_p \cdot (\Delta \mathbf{n})_L}{|\mathbf{s}_p \times \mathbf{n}_0|} \\ &= \left( \frac{\Delta b_{\pm}}{b_0} \right) \frac{\mathbf{n}_0 \times (\mathbf{r} - a_{\parallel} \mathbf{v}_c/c)}{a_{\parallel}} \cdot \frac{(\mathbf{s}_p \times \mathbf{n}_0)}{|\mathbf{s}_p \times \mathbf{n}_0|}. \end{aligned} \quad (21)$$

In general, any shift of the (co)latitude of the emission vector leads to a pulse profile variation because the pulsar radio emission is thought to be tied to a specific geometric pattern on a celestial sphere rigidly rotating around  $\mathbf{s}_p$ . Since the efficient particle acceleration leading to radio emission is thought to take place at the pulsar magnetic polar caps, the radio emission pattern is expected to be connected with the position of the pulsar magnetic axis  $\mathbf{m}$ .

Here, for illustrative purposes, we assume that the radio emission pattern forms a set of coaxial cones with circular cross sections and symmetry axes coincident with the magnetic axis  $\mathbf{m}$ , which is inclined at an angle  $\alpha$  with respect to the pulsar spin axis  $\mathbf{s}_p$  (see Fig. 3 of [9] for details of the adopted pulsar spin-magnetic geometry). This emission pattern forms the basis of the rotat-

The longitudinal time delay shifts the pulse profile uniformly in time without affecting its shape. Evaluating eq. (19) explicitly using the pulsar spin geometry described above, we find

ing vector model (RVM, see [19]) commonly adopted for inferring the pulsar spin-magnetic orientation from the pulse profile and polarization data. In the course of pulsar rotation around  $\mathbf{s}_p$ , a given emission cone is traversed by the line of sight to the observer  $\mathbf{n}_0$  only if the cone's half-opening angle  $\rho$  satisfies  $\rho > |\zeta_p - \alpha|$ . Crossing the edges of the cone by  $\mathbf{n}_0$  leads to the leading and trailing emission episodes observed at Earth.

In the RVM, the latitudinal shift  $(\Delta \zeta)_L$  [due to  $\mathbf{n}_0 \rightarrow \mathbf{n}_0 + (\Delta \mathbf{n})_L$ ] results in a variation of the full width  $2\Phi_0$  of the pulse profile (corresponding to a given emission cone), with [9]

$$\Delta \Phi_0 = - \frac{(\Delta \zeta)_L}{\sin \zeta_p \tan \chi_0}. \quad (22)$$

Here  $\chi_0$  is the angle (on the celestial sphere) between the arc connecting  $\mathbf{n}_0$  and  $\mathbf{s}_p$  and the arc connecting  $\mathbf{n}_0$  and  $\mathbf{m}$  at the edges of the pulse (see Figs. 3 & 4 of [9]). In the framework of the RVM,  $\chi_0$  is directly related to the position angle of the linear polarization of the pulsar emission, and is given by [20]

$$\tan \chi_0 = \frac{\sin \alpha \sin \Phi_0}{\cos \alpha \sin \zeta_p - \cos \Phi_0 \sin \alpha \cos \zeta_p}. \quad (23)$$

The pulse contraction/expansion  $\Delta \Phi_0$  directly translates to a *latitudinal delay* of the arrival time of various pulse *components*. This delay is  $(\Delta t)_L^{(\text{lat})} = \Delta \Phi_0 / \Omega_p$  for the leading component of the pulse profile [43]. Combining eqs. (21) and (22) we find

$$\begin{aligned} (\Delta t)_L^{(\text{lat})} &= - \frac{(\Delta \zeta)_L}{\Omega_p \sin \zeta_p \tan \chi_0} = - \left( \frac{\Delta b_{\pm}}{b_0} \right) \\ &\times \left[ \left( \frac{r}{a_{\parallel}} \right) \frac{\cos \eta_p \cos \psi + \cos i \sin \eta_p \sin \psi}{\Omega_p \sin \zeta_p \tan \chi_0} + \left( \frac{d}{a_{\parallel}} \right) \frac{\cos i \sin \eta_p (\cos \psi + e \cos \omega) - \cos \eta_p (\sin \psi + e \sin \omega)}{\Omega_p \sin \zeta_p \tan \chi_0} \right]. \end{aligned} \quad (24)$$

Setting  $d = 0$  in eq. (24) reproduces equation (23) of [9],

which was derived in the static approximation.

Since  $(\Delta t)_E^{\text{lat}}$  depends through  $\chi_0$  on phases  $\Phi_0$  of different pulse components, the latitudinal lensing time delay leads to inhomogeneous dilation/contraction of the pulse profile around the superior conjunction of the pulsar[44]. This is in contrast to the longitudinal shift of the emission vector, which only causes homogeneous displacement of the whole pulse profile in time without introducing any distortions of its shape. This difference of behaviors led [9] to propose timing of the *individual features* of the pulse profile as a means of detecting the latitudinal shift. Such a procedure yields a larger information content than the standard timing of the *whole* pulse profile (assumed to have fixed shape) which can only reveal the longitudinal time delay.

## V. FRAME-DRAGGING TIME DELAY

Frame-dragging delay  $(\Delta t)_{\text{FD}}$  owes its existence to the gravitomagnetic effect of the companion spin angular momentum  $\mathbf{S}_c$ . In order of magnitude, the metric perturbation due to  $\mathbf{S}_c$  is  $\sim S_c/r^2$  (in units where  $G = c = 1$ ), the additional time delay for a ray with impact parameter  $b$  is then  $(\Delta t)_{\text{FD}} \sim S_c/b$ . Given the small magnitude of this delay, in its subsequent consideration we will neglect the effect of the companion motion and will use static approximation accounting only for lensing effects. We have (see e.g., [12])

$$(\Delta t)_{\text{FD}} = -\frac{2G}{c^4} \int d\mathbf{r}_{ph} \cdot \frac{\mathbf{S}_c \times (\mathbf{r}_{ph} - \mathbf{r}_c)}{|\mathbf{r}_{ph} - \mathbf{r}_c|^3}, \quad (25)$$

where  $\mathbf{r}_{ph}$  is the position vector for the photon trajectory (see also Appendix A). Assuming that the observer is at infinite distance from the system and evaluating the integral in (25) we find

$$(\Delta t)_{\text{FD}} = -\frac{2G}{c^4} \frac{\mathbf{n}_0 \cdot (\mathbf{S}_c \times \mathbf{R})}{b_{\pm} R} \left[ 1 + \frac{r_{\parallel}}{(r_{\parallel}^2 + b_{\pm}^2)^{1/2}} \right]. \quad (26)$$

As  $(\Delta t)_{\text{FD}}$  may only be noticeable in nearly edge-on systems and at the conjunction, one can use  $b_{\pm} \ll r_{\parallel}$ . We specify the orientation of the companion's spin vector  $\mathbf{S}_c$  by the angles  $\zeta_c$  and  $\eta_c$  (analogous to angles  $\zeta_p$  and  $\eta_p$  used to describe the orientation of  $\mathbf{s}_p$ ) and its magnitude by the dimensionless spin parameter  $\tilde{a} \leq 1$  according to

$$S_c = \tilde{a} \frac{GM_c^2}{c}. \quad (27)$$

We then find

$$\begin{aligned} (\Delta t)_{\text{FD}} &= -(\Delta t)_{\text{FD}}^{\text{max}} \tilde{a} \sin \zeta_c \left( \frac{R_E}{b_{\pm}} \right) \\ &\times \frac{\sin \eta_c \cos \psi - \cos \eta_c \sin \psi \cos i}{(1 - \sin^2 \psi \sin^2 i)^{1/2}} \end{aligned} \quad (28)$$

where we have introduced a fiducial unit of time

$$\begin{aligned} (\Delta t)_{\text{FD}}^{\text{max}} &= \frac{R_g^2}{cR_E} = \frac{R_g}{c} \left( \frac{R_g}{2a_{\parallel}} \right)^{1/2} \\ &\approx 1.44 \times 10^{-2} \mu\text{s} \left( \frac{M_c}{M_{\odot}} \right)^{3/2} \left( \frac{R_{\odot}}{a_{\parallel}} \right)^{1/2}. \end{aligned} \quad (29)$$

Note that  $(\Delta t)_{\text{FD}}$  never diverges, not even for  $\Delta i = 0$ . If one were to neglect the light deflection by the companion (as has been done in all previous studies, see [11], [12], [13], [14]),  $(\Delta t)_{\text{FD}}$  would still be given by equation (26) but with  $R$  instead of  $b_{\pm}$ . This would lead to a divergent  $(\Delta t)_{\text{FD}}$  as  $i \rightarrow \pi/2$  and  $\psi \rightarrow \pi/2$ . In the limit  $R \gg R_E$ , eq. (28) reduces to the corresponding result of [12] obtained neglecting lensing.

From eq. (28), it is clear that  $(\Delta t)_{\text{FD}}^{\text{max}}$  is the *maximum possible* value of the frame-dragging time delay since  $b_{+} \geq R_E$ . This fundamental limit may be approached if the companion is a maximally spinning black hole with a certain spin orientation and  $i = \pi/2$ ,  $\psi = \pi/2$ . Note that for the negative image,  $b_{-} \leq R_E$  and  $(\Delta t)_{\text{FD}}$  exceeds  $(\Delta t)_{\text{FD}}^{\text{max}}$  roughly by  $R_E/b_{-}$ , (neglecting various geometric factors and assuming  $\tilde{a} = 1$ ), but its magnification  $A_{-} = (b_{-}/R_E)^4/[1 - (b_{-}/R_E)^4]$  rapidly goes to zero as the time delay increases. Thus, observations of the negative image are not feasible in practice.

## VI. APPLICATION TO HIGHLY-INCLINED SYSTEMS

The effects of gravitational lensing and companion motion discussed in previous sections are of interest only for nearly edge-on binaries, those with  $|\Delta i| = |i - \pi/2| \ll 1$ . In particular, for the ‘‘strong-lensing’’ systems (those with  $|\Delta i| \lesssim R_E/a_{\parallel}$ ), the image shift at the orbital conjunction ( $\psi = \pi/2$ ),  $\Delta b \sim R_E \sim a_{\parallel} v/c$ , is of the same order as the apparent change of the photon impact parameter due to the companion motion,  $|\mathbf{b}_0 - \mathbf{R}| = a_{\parallel} V_c/c$  [see eq. (5)]. Therefore it is important to account for both lensing and companion motion properly for such systems.

### A. Effect of Companion Motion

For a highly inclined binary system ( $|\Delta i| \ll 1$ ) around the orbital conjunction ( $|\Delta \psi = |\psi - \pi/2| \ll 1$ ), the effect of lens motion on the various time delays studied in previous sections has a simple interpretation, as we now show. Expanding eq. (6) for  $|\Delta i|, |\Delta \psi| \ll 1$ , we find

$$\begin{aligned} b_0 &\simeq a_{\parallel} \left\{ [\Delta \psi + (d/a_{\parallel})(1 + e \sin \omega)]^2 \right. \\ &\quad \left. + (\Delta i)^2 [1 + (d/a_{\parallel})e \cos \omega]^2 \right\}^{1/2} \\ &\simeq a_{\parallel} \left\{ [\Delta \psi + (d/a_{\parallel})(1 + e \sin \omega)]^2 + (\Delta i)^2 \right\}^{1/2} \end{aligned} \quad (30)$$

Comparing with the static limit,  $b_0^{(\text{stat})} = R \simeq a_{\parallel} [(\Delta\psi)^2 + (\Delta i)^2]^{1/2}$ , we see that  $b_0|_{\psi} \simeq b_0^{\text{stat}}|_{\psi+\Delta\psi_{\text{ret}}}$ , where we have introduced a phase shift

$$\Delta\psi_{\text{ret}} \equiv \frac{d}{a_{\parallel}}(1 + e \sin \omega) = \frac{\Omega_b a_c}{c} \frac{(1 + e \sin \omega)}{\sqrt{1 - e^2}}. \quad (31)$$

Clearly, in the presence of the lens motion, the photon impact parameter is minimal not at  $\Delta\psi = 0$  (exact conjunction) but at  $-\Delta\psi_{\text{ret}}$ , which occurs slightly *before* the conjunction. This is a direct manifestation of the retardation effect due to the finite time it takes for the photons emitted by the pulsar to propagate through the binary, during which the lensing companion's position changes (see [10], [21]).

As mentioned in §III, near the conjunction the Shapiro delay  $(\Delta t)_{\text{grav}}$  is described by eq. (16). It is then obvious from (12) and (16) that lens motion affects  $(\Delta t)_{\text{grav}}$  and  $(\Delta t)_{\text{geom}}$  only through its effect on  $b_0$  which enters  $b_{\pm}$  in these formulae. Thus,

$$\begin{aligned} (\Delta t)_{\text{grav}}|_{\psi} &\simeq (\Delta t)_{\text{grav}}^{\text{stat}}|_{\psi+\Delta\psi_{\text{ret}}}, \\ (\Delta t)_{\text{geom}}|_{\psi} &\simeq (\Delta t)_{\text{geom}}^{\text{stat}}|_{\psi+\Delta\psi_{\text{ret}}}, \end{aligned} \quad (32)$$

for  $|\Delta i|, |\Delta\psi| \ll 1$ , where  $(\Delta t)_{\text{grav}}^{\text{stat}}$  and  $(\Delta t)_{\text{geom}}^{\text{stat}}$  are the Shapiro and geometric delays calculated in the static limit [8].

For the spin-dependent time delays near conjunction, one finds using eqs. (20) and (24)

$$\begin{aligned} (\Delta t)_L &\simeq - \left( \frac{\Delta b_{\pm}}{b_0} \right) \\ &\frac{\cos \eta_p \Delta i - \sin \eta_p [\Delta\psi + (d/a_{\parallel})(1 + e \sin \omega)]}{\Omega_p \sin \zeta_p}, \end{aligned} \quad (33)$$

$$\begin{aligned} (\Delta t)_L^{(\text{lat})} &\simeq - \left( \frac{\Delta b_{\pm}}{b_0} \right) \\ &\frac{\sin \eta_p \Delta i + \cos \eta_p [\Delta\psi + (d/a_{\parallel})(1 + e \sin \omega)]}{\Omega_p \sin \zeta_p \tan \chi_0}. \end{aligned} \quad (34)$$

It is again clear that

$$\begin{aligned} (\Delta t)_L|_{\psi} &\simeq (\Delta t)_L^{\text{stat}}|_{\psi+\Delta\psi_{\text{ret}}}, \\ (\Delta t)_L^{(\text{lat})}|_{\psi} &\simeq (\Delta t)_L^{(\text{lat},\text{stat})}|_{\psi+\Delta\psi_{\text{ret}}}, \end{aligned} \quad (35)$$

where  $(\Delta t)_L^{\text{stat}}$  and  $(\Delta t)_L^{(\text{lat},\text{stat})}$  are the longitudinal and latitudinal light-bending delays calculated in the static approximation ([9]).

Equations (32) and (35) show that all delays discussed here are related to their static analogs via  $(\Delta t)(\psi) \simeq (\Delta t)^{\text{stat}}(\psi + \Delta\psi_{\text{ret}})$  for  $|\Delta i|, |\Delta\psi| \ll 1$ . Thus, the effect of the companion motion is to simply *shift* the delay curves  $(\Delta t)^{\text{stat}}(\psi)$  homogeneously in phase by  $-\Delta\psi_{\text{ret}}$  without affecting the amplitude or shape of these curves (to  $v/c$  accuracy). This phase shift is equivalent to moving the time delay curves calculated in the static approximation *earlier* in time by

$$\Delta t_{\text{ret}} = \frac{\Delta\psi_{\text{ret}}}{\Omega_b} \frac{(1 - e^2)^{3/2}}{(1 + e \sin \omega)^2} = \frac{M_p a}{M c} \frac{1 - e^2}{1 + e \sin \omega}. \quad (36)$$

One can see that as advertised in §I this time shift is indeed equal to  $(M_p/M)a_{\parallel}/c$ , i.e., the light crossing time of the binary at conjunction weighted by the mass ratio  $M_p/M$ .

To illustrate our results, consider the double pulsar J0737-3039 system, consisting of the millisecond pulsar A with spin period  $P_A = 22.7$  ms and mass  $M_p = 1.337M_{\odot}$ , and the normal pulsar B with mass  $M_c = 1.25M_{\odot}$  playing the role of the lensing companion ([22], [3]). This nearly edge-on system has  $P_b = 0.1023$  d,  $e = 0.0878$ , and  $a = 8.784 \times 10^{10}$  cm. The phase shift is  $\Delta\psi_{\text{ret}} \approx 1.2 \times 10^{-3}$ , and time shift  $\Delta t_{\text{ret}} \approx 1.4$  s. In Fig. 1 we display the timing delays discussed in this paper for J0737-3039 – the combined geometric and Shapiro delays given by eqs. (12) and (14), and the rotational lensing delays given by eqs. (20) and (24) – together with the image magnification factor given by eq. (11), which depends on  $b_0$  and is thus also affected by the lens motion. We choose  $i = 90.29^\circ$  ([23]) for this figure, which allows lensing effects to manifest themselves (see [8], [9]). To evaluate the spin-dependent delays  $(\Delta t)_L$  and  $(\Delta t)_L^{(\text{lat})}$ , we adopt as an example  $\zeta = 50^\circ$ ,  $\eta = 45^\circ$  consistent with the polarization measurement of [24]. Compared to the static results, all these curves are shifted back in time from the moment of conjunction.

Although the example in Fig. 1 refers to the “strong lensing” case ( $|\Delta i| \lesssim v/c$ ), we emphasize that for any highly-inclined system ( $|\Delta i| \ll 1$ ), the effect of the companion motion can be captured adequately by the “retardation shift” as described above. In Table I we list  $\Delta\psi_{\text{ret}}$  and  $\Delta t_{\text{ret}}$  for binary pulsar systems with measured Shapiro delays. One can see that the value of  $\Delta t_{\text{ret}}$  ranges from several seconds in compact systems to several minutes in wide binaries. Detection of the retardation effect seems easier for the latter but would ultimately depend on the accuracy of timing observations of a given system[45].

## B. Effect of Frame-Dragging

Previous conclusions on the observability of the frame-dragging time delay have been over-optimistic as they have always been obtained neglecting the light bending effect. For example, for a binary pulsar system with  $M_c = 10 M_{\odot}$ ,  $\tilde{a} = 1$ , and  $a_{\parallel} \approx 9.4 R_{\odot}$  (corresponding to binary period of 1 d), Wex & Kopeikin [12] found that  $(\Delta t)_{\text{FD}}$  reaches  $1 \mu\text{s}$  for  $|i - \pi/2| \approx 0.05^\circ$ , while our eq. (29) gives  $(\Delta t)_{\text{FD}}^{\text{max}} \approx 0.15 \mu\text{s}$ . This difference is easily understood by noticing that for this set of parameters,  $R_E \approx 2 \times 10^4$  km is considerably larger than the assumed unperturbed impact parameter of the radio beam,  $a_{\parallel}|i - \pi/2| \approx 5.7 \times 10^3$  km. Thus, light bending cannot be neglected in the calculation of  $(\Delta t)_{\text{FD}}$  for this system. For binary pulsars with neutron star companions,  $(\Delta t)_{\text{FD}}$  is completely negligible (contrary to the claims in Refs. [13] and [14]).

Another problem with stellar-mass binaries is that

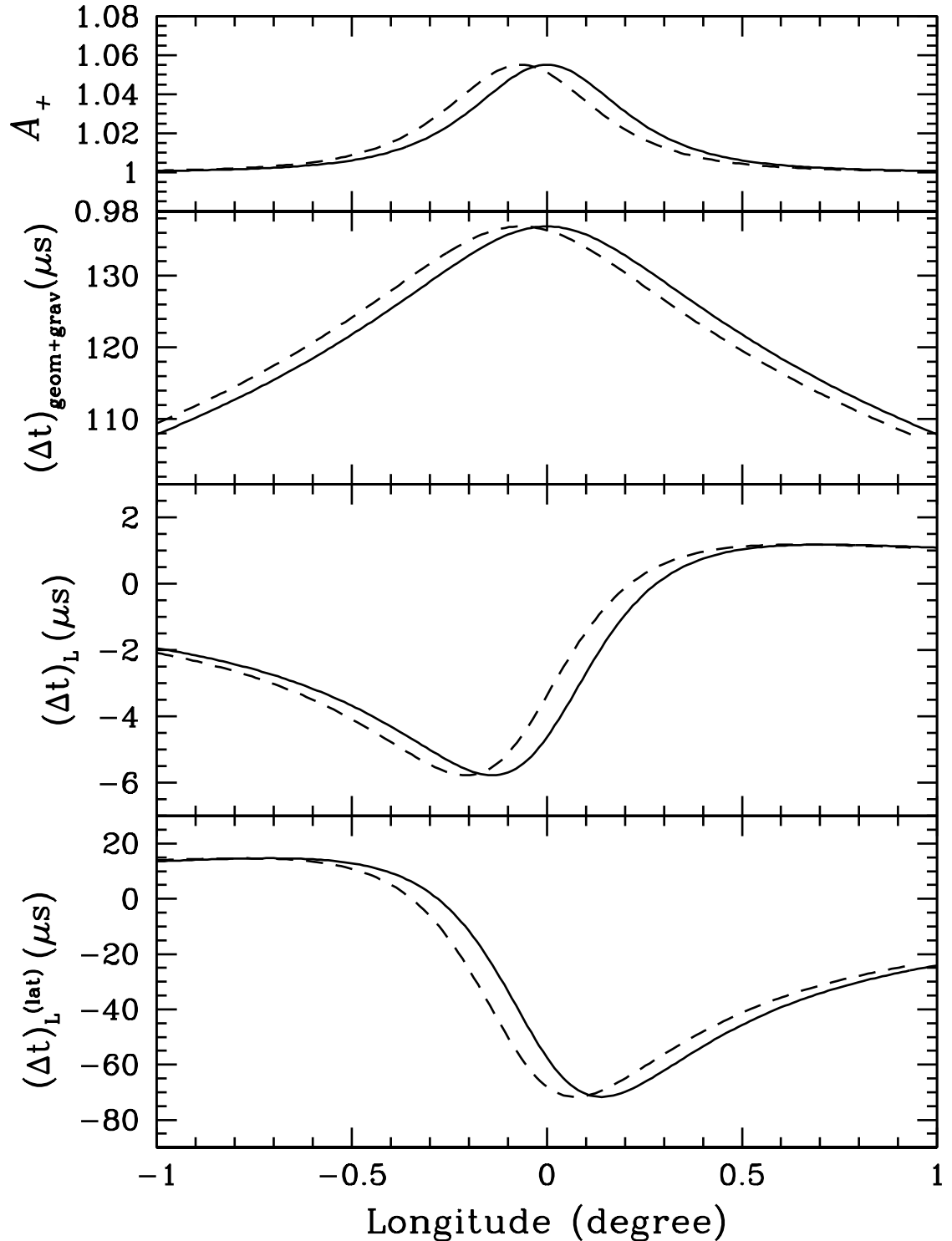


FIG. 1: The amplification (top panel), the combined geometric and Shapiro delay (the second panel), the rotational-lensing delay (the third panel), and the latitudinal lensing delay (the bottom panel) of the dominant (“plus”) image of the pulsar A signal as a function of the orbital phase in the double pulsar PSR J0737-3039 system. The longitude is measured from the superior conjunction of pulsar A (when A is exactly behind pulsar B). The inclination angle is chosen to be  $90.29^\circ$ . For the third and bottom panels, the angles  $\zeta = 50^\circ$ ,  $\eta = 45^\circ$  and  $\tan \chi_0 = 0.08$  are used. In each panel, the solid curve corresponds to the static limit (see Fig. 1 of [9]), while the dashed curve includes the effect of the companion motion.

TABLE I: Binary pulsars with measured Shapiro delays.

PSR	$P_p^a$ , ms	$P_b^b$ , d	$a/c$ , s	$M_c$ , $M_\odot$	$\sin i$	$\Delta\psi_{\text{ret}}$	$\Delta t_{\text{ret}}$ , s	Ref.
B1534+12 <sup>c</sup>	37.9	0.42	7.6	1.345	0.975	$9.2 \times 10^{-4}$	8.87	[25]
J0737-3039 <sup>c</sup>	22.7	0.1	2.93	1.25	0.999987 <sup>e</sup>	$11.8 \times 10^{-4}$	1.39	[3]
B1855+09 <sup>d</sup>	5.4	12.3	60	0.23	0.9995	$3 \times 10^{-4}$	50.8	[26]
J0437-4715 <sup>d</sup>	5.8	5.7	37.6	0.24	0.679	$4.2 \times 10^{-4}$	32.6	[27]
J1713+0747 <sup>d</sup>	4.57	67.8	192	0.28	0.9	$1.7 \times 10^{-4}$	158	[4]
J1640+2224 <sup>d</sup>	3.16	175.5	369	0.25	0.99	$1.3 \times 10^{-4}$	313	[28]
J1909-3744 <sup>d</sup>	2.95	1.53	15.3	0.2	0.998	$6.4 \times 10^{-4}$	13.4	[5]
J0751+1807 <sup>d</sup>	3.4	0.26	5.8	0.19	0.83	$14.9 \times 10^{-4}$	5.32	[29]

<sup>a</sup>Pulsar spin period,  $P_p = 2\pi/\Omega_p$ .

<sup>b</sup>Orbital period of the binary,  $P_b = 2\pi/\Omega_b$ .

<sup>c</sup>Pulsar companion is a neutron star.

<sup>d</sup>Pulsar companion is a white dwarf.

<sup>e</sup>Value of  $\sin i$  from scintillation measurements of [23]. Shapiro delay suggests  $\sin i = 0.9997$  [30].

$(\Delta t)_{\text{FD}}$  is degenerate with the longitudinal lens-rotational delay  $(\Delta t)_L$ . This was first pointed out in [12] under the weak light bending approximation [46], but it is easy to see that this degeneracy holds even in the case of strong lensing:  $\Delta b_\pm$  satisfies the lens equation  $\Delta b_\pm = R_E^2/b_\pm$ , and the  $\psi$ -dependent factors in eqs. (20) and (28) are analogous [47] (the only difference is in  $\eta_p$  used in the former and  $\eta_c$  in the latter). As a result, these two delays are covariant and in practice it is not possible to separate their contributions unless there exists some additional information on their relative magnitudes such as the knowledge of the pulsar spin-magnetic orientation from polarization measurements.

These examples lead us to conclude that measuring frame-dragging effect in the stellar mass pulsar binaries is impossible if the timing precision is to remain at the level of  $1 \mu\text{s}$ . In principle, shrinking binary (reducing  $a_\parallel$ ) boosts up  $(\Delta t)_{\text{FD}}^{\text{max}}$ , but this comes at the cost of reducing the binary lifetime due to gravitational wave emission [11]. If a pulsar is found around a high-mass black hole (such as the one in the Galactic Center, see [31]) in a highly inclined orbit, the chance of measuring frame-dragging delay may be better: in this case  $(\Delta t)_{\text{FD}}^{\text{max}}$  not only is large but also strongly exceeds  $(\Delta t)_L$ .

## VII. DISCUSSION

In this paper we have studied the combined effects of gravitational lensing and companion motion on various time delays in binary pulsar systems. Our study improves upon previous work on the lensing effect by going beyond the static approximation ([8], [9]). We show that for highly inclined systems, the companion motion affects the Shapiro delay and other lensing-related delays by shifting the delay curves backward in time by the amount  $\sim a_c/c$  (where  $a_c$  is the semimajor axis of the companion).

To detect this effect on time delays, one should look for a systematic displacement of the peak of the Shapiro delay curve from the exact moment of the superior conjunction of the pulsar. To this end, one must be able to pinpoint the exact moment of the conjunction and to nail down the peak of the Shapiro delay curve. This may not be so easy since in practice one bins the timing data within rather large time intervals to get a good measurement of the Shapiro delay. Thus, one would need repeated measurements of many binary pulsar orbits to be able to reach the accuracy needed for measuring the retardation effect. Retardation effect on lensing delays *may* be detectable in the double pulsar system J0737-3039, but the feasibility of this measurement depends on the currently uncertain inclination of the system and is compromised by the eclipse of the millisecond pulsar near its superior conjunction by the magnetosphere of its companion ([3], [32]).

In the case of the double pulsar J0737-3039 system, the retardation effect due to the companion motion not only affects timing of the millisecond pulsar but may also influence the interpretation of the scintillation measurements of this system near conjunction [23]. Indeed, the correlated measurements of the interstellar scintillations of the two pulsars provide information about the system orientation and properties of the interstellar turbulence only when the positions of both pulsar projected on the sky plane are accurately known at each moment of time. In the static approximation the projected separation of pulsars is  $\mathbf{R}$ , while it becomes  $\mathbf{b}_0$  [see eq. (5)] when the retardation effect is taken into account. For the currently inferred inclination angle from the scintillation measurement itself ( $|i - 90^\circ| = 0.29^\circ \pm 0.14^\circ$ , [23]), both the retardation effect and the light bending distortion of the apparent path of the lensed millisecond pulsar [8] have similar orders of magnitudes and contribute at the level of  $\sim R_E$  to the projected pulsar separation at conjunction. As for this system  $R_E = 2550 \text{ km}$  is not



very different from the inferred minimum projected approach distance of the two pulsars,  $\approx 4000 \pm 2000$  km, one expects that both effects may at some level affect the interpretation of the correlated scintillation measurements of [23]. Whether this can explain the discrepancy between the values of the system's inclination obtained using the Shapiro delay ( $i = 88.7^\circ \pm 0.9^\circ$ ; [3], [33]) and scintillations is not clear at present.

### Acknowledgments

RRR thankfully acknowledges the financial support by the Canada Research Chairs Program. DL thanks Saul Teukolsky for discussion, and is supported in part by NSF grant AST 0307252 and NASA grant NAG 5-12034.

## APPENDIX A: FORMAL DERIVATION OF THE SHAPIRO DELAY FORMULA FOR MOVING LENS

The metric produced by the companion (mass  $M_c$ ) in its rest frame (“primed” frame) assumes the standard form (we set  $G = c = 1$  in this appendix)

$$ds^2 = -(1 + 2\Phi)(dt')^2 + (1 + 2\Phi)^{-1}d\mathbf{x}' \cdot d\mathbf{x}', \quad (\text{A1})$$

where  $\Phi = -M_c/|\mathbf{x}'|$ , and  $\mathbf{x}'$  is the 3-vector measured from  $M_c$ . In the “lab” frame (“unprimed”) comoving with the barycenter of the binary, where the lens moves with velocity  $\mathbf{v}_c$ , the metric can be obtained by a Lorentz boost. To order  $\mathcal{O}(v_c)$ , it is given by

$$ds^2 = -(1 + 2\Phi)dt^2 + 8\Phi \mathbf{v}_c \cdot d\mathbf{x}dt + (1 - 2\Phi)d\mathbf{x} \cdot d\mathbf{x}. \quad (\text{A2})$$

The above result can also be obtained using the linearized theory of gravity (e.g., [34]): The metric coefficients produced by a source with density  $\rho(t, \mathbf{x})$  and velocity  $\mathbf{v}(t, \mathbf{x})$  are

$$g_{00} = -1 + 2U + \mathcal{O}(\epsilon^2), \quad (\text{A3})$$

$$g_{0i} = -4V_i + \mathcal{O}(\epsilon^{5/2}), \quad (\text{A4})$$

$$g_{ij} = \delta_{ij}(1 + 2U) + \mathcal{O}(\epsilon^2), \quad (\text{A5})$$

where  $\epsilon \sim \mathcal{O}(v_c^2, M_c/r)$ , and

$$U = \int \frac{\rho(t - |\mathbf{x} - \mathbf{x}'|/c, \mathbf{x}')}{|\mathbf{x} - \mathbf{x}'|} d^3x', \quad (\text{A6})$$

$$V_i = \int \frac{\rho \mathbf{v}_c(t - |\mathbf{x} - \mathbf{x}'|/c, \mathbf{x}')}{|\mathbf{x} - \mathbf{x}'|} d^3x'. \quad (\text{A7})$$

Taylor expansions show that the retardation effect enters the potentials only in the order  $\mathcal{O}(v_c^2)$ , and eq. (A2) is recovered (e.g., [17]).

Let the position vector of the companion (lens) be  $\mathbf{r}_c(t)$ , and that of the ray be  $\mathbf{r}_{\text{ph}}(t)$ . Along the ray, the potential  $\Phi = -M_c/|\mathbf{x}'|$  should be evaluated at

$$\mathbf{x}' = \mathbf{r}'_{\text{ph}}(t') - \mathbf{r}'_c(t') \simeq \mathbf{r}_{\text{ph}}(t) - \mathbf{r}_c(t). \quad (\text{A8})$$

A Lorentz transformation shows that the correction to eq. (A8) is of order  $\mathcal{O}(v_c^2)$  and will be neglected. The photon trajectory  $\mathbf{r}_{\text{ph}}(t)$  satisfies  $ds^2 = 0$ , which gives

$$dt = [1 - 2\Phi(1 - 2\mathbf{v}_c \cdot \mathbf{k})] dl, \quad (\text{A9})$$

where  $d\mathbf{r}_{\text{ph}} = dl \mathbf{k}$  (with  $\mathbf{k}$  the unit vector of photon propagation) and  $dl = (d\mathbf{r}_{\text{ph}} \cdot d\mathbf{r}_{\text{ph}})^{1/2}$ . This corresponds to an effective index of refraction  $1 + (2M_c/|\mathbf{x}'|)(1 - 2\mathbf{v}_c \cdot \mathbf{k})$  (e.g., [35]).

Consider a photon emitted from the source (the pulsar) at time  $t_e$  (near the binary conjunction), and arriving to the observer at  $t_o$ . The impact parameter of the photon is  $b = b_0 + \Delta b$  [see eq. (13)]. Integration of eq. (A9) along the ray path yields

$$t_o - t_e = |\mathbf{r}_{\text{ph}}(t_o) - \mathbf{r}_{\text{ph}}(t_e)| + (\Delta t)_{\text{geom}} + (\Delta t)_{\text{grav}}, \quad (\text{A10})$$

where the 1st term gives the usual Roemer delay, the 2nd term is the geometric delay given by equation (12), and the 3rd term is the Shapiro delay represented by

$$(\Delta t)_{\text{grav}} = \int dl \frac{2M_c}{|\mathbf{x}'|} (1 - 2\mathbf{v}_c \cdot \mathbf{k}), \quad (\text{A11})$$

where the integration is along the ray path and  $\mathbf{x}' = \mathbf{r}'_{\text{ph}}(t') - \mathbf{r}'_c(t') \simeq \mathbf{r}_{\text{ph}}(t) - \mathbf{r}_c(t)$ .

Without loss of generality, let us assume that the photon passes through the lens plane at  $t = t_l = 0$ . Then the photon position vector is  $\mathbf{r}_{\text{ph}}(t) = \mathbf{r}_{\text{ph}}(0) + ct\mathbf{k}$ , with  $\mathbf{k} = \mathbf{n}_0$  for  $t > 0$  and  $\mathbf{k} = \mathbf{n} = \mathbf{n}_0 + \Delta\mathbf{n}$ , where  $\mathbf{n}_0$  is the unit vector pointing toward the observer and  $\Delta\mathbf{n} = \Delta\mathbf{b}/a_{\parallel}$ . The lens position vector is  $\mathbf{r}_c = \mathbf{r}_c(0) + \mathbf{v}_c t = \mathbf{r}_c(0) + \mathbf{V}_c t + v_{\parallel} t \mathbf{n}_0$ , where  $v_{\parallel} = \mathbf{n}_0 \cdot \mathbf{v}_c$ , and  $\mathbf{V}_c$  is the projection of  $\mathbf{v}_c$  on the sky plane. Thus, along the ray  $\mathbf{x}' = (\mathbf{b} - \mathbf{V}_c t + \sigma c \Delta\mathbf{n} t) + (c - v_{\parallel}) t \mathbf{n}_0$ , with  $\sigma = 1$  for  $t < 0$  and  $\sigma = 0$  for  $t > 0$ , and  $\mathbf{b} = \mathbf{b}_{\pm} = \mathbf{r}_{\text{ph}}(0) - \mathbf{r}_c(0)$ . Taking the integral in (A11) we have to order  $v_c^2$

$$\begin{aligned} \Delta t_1 &= 2M_c(1 + v_{\parallel}) \ln \left( s + \sqrt{s^2 + b^2} \right) \Big|_{s=-\mathbf{b} \cdot \mathbf{V}_c}^{s=s_o(1-v_{\parallel})-\mathbf{b} \cdot \mathbf{V}_c} \\ &+ 2M_c(1 + v_{\parallel}) \\ &\times \ln \left( s + \sqrt{s^2 + b^2} \right) \Big|_{s=s_e(1-v_{\parallel})-\mathbf{b} \cdot (\mathbf{V}_c - c\Delta\mathbf{n})}^{s=-\mathbf{b} \cdot (\mathbf{V}_c - c\Delta\mathbf{n})}, \end{aligned} \quad (\text{A12})$$

where  $s_e = ct_e$ ,  $s_o = ct_o$ . Since  $s_o \rightarrow \infty$ , the upper limit only amounts to a constant which can be dropped. Thus to leading order

$$\begin{aligned} \Delta t_1 &= -2M_c(1 + v_{\parallel}) \\ &\times \ln \left( s + \sqrt{s^2 + b^2} \right)_{s=s_e(1-v_{\parallel})-\mathbf{b} \cdot (\mathbf{V}_c - c\Delta\mathbf{n})} \end{aligned} \quad (\text{A13})$$

Note that  $s_e = ct_e$  is determined by  $\mathbf{n}_0 \cdot [\mathbf{r}_p(t_e) + (0 - t_e)c\mathbf{n}] = \mathbf{n}_0 \cdot \mathbf{r}_c(0) = \mathbf{n}_0 \cdot [\mathbf{r}_c(t_e) - \mathbf{v}_c t_e]$ , which gives  $s_e = ct_e = -(1 + v_{\parallel}) r_{\parallel}$ , where  $r_{\parallel} = -\mathbf{n}_0 \cdot \mathbf{r}(t_e)$  and  $\mathbf{r} = \mathbf{r}_p - \mathbf{r}_c$ . Thus the Shapiro delay  $(\Delta t)_{\text{grav}} =$

$(1 - 2v_{\parallel})\Delta t_1$  is given by

$$\begin{aligned}
 (\Delta t)_{\text{grav}} = & -2M_c(1 - \mathbf{n}_0 \cdot \mathbf{v}_c) \\
 & \times \ln \left[ \sqrt{(r_{\parallel} + \mathbf{b} \cdot \mathbf{V}_c - c\mathbf{b} \cdot \Delta \mathbf{n})^2 + b^2} \right. \\
 & \left. - r_{\parallel} - \mathbf{b} \cdot \mathbf{V}_c + \mathbf{b} \cdot \Delta \mathbf{n} \right], \quad (\text{A14})
 \end{aligned}$$

where all quantities are evaluated at  $t = t_e$ .

There are some differences between eq. (A14) and eq. (14) (apart from the trivial additive constant term

in the latter). These differences appear in the expression inside the logarithm, and are of order  $(v_c/c)^2$ . This is expected since our calculation includes only the leading-order  $v_c/c$  correction to the “static” Shapiro delay formula, while higher-order terms are neglected. Indeed, it is easy to show that eq. (A14) reduces to eqs. (15) or (16) in the appropriate limits. We conclude that both eqs. (14) and (A14) give the same  $v_c/c$  corrections to the Shapiro delay, and they should in practice give the same quantitative result for  $(\Delta t)_{\text{grav}}$ .

- 
- [1] I. Stairs, S. E. Thorsett, and Z. Arzoumanian, *Phys. Rev. Lett.* **93**, 141101 (2004).
- [2] A. W. Hotan, M. Bailes, and S. M. Ord, *ApJ* **624**, 906 (2005).
- [3] A. G. Lyne and et al. , *Science* **303**, 1153 (2004).
- [4] E. M. Splaver and et al. , *ApJ* **620**, 405 (2005).
- [5] B. A. Jacoby and et al. , *ApJ* **629**, L113 (2005).
- [6] J. Schneider, *A&A* **232**, 62 (1990).
- [7] O. V. Doroshenko and S. M. Kopeikin, *MNRAS* **274**, 1029 (1995).
- [8] D. Lai and R. R. Rafikov, *ApJ* **621**, L41 (2005).
- [9] R. R. Rafikov and D. Lai, *ApJ to appear*, **astro-ph/0503461** (2006).
- [10] S. M. Kopeikin and G. Schafer, *Phys. Rev. D* **60**, 124002 (1999).
- [11] P. Laguna and A. Wolszczan, *ApJ* **486**, L27 (1997).
- [12] N. Wex and S. M. Kopeikin, *ApJ* **514**, 388 (1999).
- [13] A. Tartaglia, M. L. Ruggiero, and A. Nagar, *Phys. Rev. D* **71**, 023003 (2005).
- [14] M. L. Ruggiero and A. Tartaglia, *Phys. Rev. D* **72**, 084030 (2005).
- [15] T. Pyne and M. Birkinshaw, *ApJ* **415**, 459 (1993).
- [16] O. Wucknitz and U. Spherhake, *Phys. Rev. D* **69**, 063001 (2004).
- [17] C. C. Will, *ApJ* **590**, 683 (2003).
- [18] T. Damour and J. H. Taylor, *Phys. Rev. D* **45**, 1840 (1992).
- [19] V. Radhakrishnan and D. Cooke, *ApJ* **3**, 225 (1969).
- [20] M. M. Komesaroff, *Nature* **225**, 612 (1970).
- [21] S. M. Kopeikin, *Radio Pulsars, ASP Conference Proceedings, 302* (Astronomical Society of the Pacific, San Francisco, 2003).
- [22] M. Burgay, N. D’Amico, A. Possenti, and et al. , *Nature* **426**, 531 (2003).
- [23] W. A. Coles, M. A. McLaughlin, B. J. Rickett, and et al. , *ApJ* **623**, 392 (2005).
- [24] P. Demorest and et al. , *ApJ* **615**, L137 (2004).
- [25] I. Stairs and et al. , *ApJ* **581**, 501 (2002).
- [26] M. F. Ryba and J. H. Taylor, *ApJ* **371**, 739 (1991).
- [27] W. van Straten and et al. , *Nature* **412**, 158 (2001).
- [28] O. Lohmer and et al. , *ApJ* **621**, 388 (2005).
- [29] D. Nice and et al. , *ApJ* **634**, 1242 (2005).
- [30] V. Kaspi, S. Ransom, D. G. Backer, and et al. , *ApJ* **613**, L137 (2004).
- [31] E. Pfahl and A. Loeb, *ApJ* **615**, 253 (2004).
- [32] M. A. McLaughlin and et al. , *ApJ* **613**, L53 (2004).
- [33] S. Ransom and et al. , *ApJ* **609**, L71 (2004).
- [34] C. Misner, K. S. Thorne, and J. A. Wheeler, *Gravitation* (W. H. Freeman, New York, 2003).
- [35] P. Schneider, J. Ehlers, and E. E. Falco, *Gravitational Lenses* (Springer-Verlag, Berlin, 1992).
- [36] R. Blandford and S. A. Teukolsky, *ApJ* **205**, 580 (1976).
- [37] L. L. Smarr and R. Blandford, *ApJ* **207**, 574 (1976).
- [38] T. Damour and N. Deruelle, *Ann. Inst. Henri Poincaré* **44**, 263 (1986).
- [39] Although  $v_c$  is not constant, as long as the orbital period of the system is longer than the photon propagation time across the binary, the companion’s acceleration can be neglected, see [10].
- [40] Note that we include the constant term  $(R_g/c) \ln [a(1 - e^2)]$  in eq. (14) so that in the static, no-lensing limit it reduces to the conventional expression (e.g., [36])
- $$(\Delta t)_{\text{grav}} = (R_g/c) \ln \left[ \frac{1 + e \cos \phi}{1 - \sin i \sin(\phi + \omega)} \right].$$
- [41] The negative image is highly demagnified and is unobservable.
- [42] The subscript “L” in  $(\Delta \mathbf{n})_L$  serves as a reminder that the effect is due to lensing. The orbital motion of the pulsar also gives rise to aberration of the emission direction in the pulsar’s rest frame; such “aberration delays” ([37], [38], [9]) are not affected directly by the motion of the companion, and are not discussed in this paper.
- [43] For the trailing component, the latitudinal delay is  $-\Delta\Phi_0/\Omega_p$ . Hereafter our formulae refer to the leading component.
- [44] Although our formulae are based on the RVM, similar latitudinal pulse shape variation and delays should be exhibited by all non-pathological emission patterns, not just that assumed by the RVM.
- [45] For PSR J1909-3744 timing residuals may become as low as 10 ns [5] which should make it one of the best systems to probe the retardation effect even though its  $\Delta t_{\text{ret}}$  is only 13 s.
- [46] Their calculation of  $(\Delta t)_L$  was in the weak lensing regime while the expression for  $(\Delta t)_{\text{FD}}$  neglected lensing altogether.
- [47] One needs to set  $d = 0$  and  $b_0 \rightarrow R = r(1 - \sin^2 \psi \sin^2 i)^{1/2}$  in (20) as eq. (28) was derived in the static limit.